Secondary Structure and Interactions of the Packaged dsDNA Genome of Bacteriophage P22 Investigated by Raman Difference Spectroscopy†

K. L. Aubrey,‡ S. R. Casjens,§ and G. J. Thomas, Jr.*,‡

Division of Cell Biology and Biophysics, School of Biological Sciences, University of Missouri—Kansas City, Kansas City, Missouri 64110-2499, and Department of Cellular, Viral and Molecular Biology, University of Utah Medical Center, Salt Lake City, Utah 84132

Received May 15, 1992; Revised Manuscript Received August 25, 1992

ABSTRACT: Vibrational spectra of the double-stranded DNA genome of bacteriophage P22 in packaged and unpackaged states are compared by digital difference Raman spectroscopy. The difference Raman spectrum, which is sensitive to structural changes at the level of <2% of a given nucleotide type, reveals the effects of packaging upon sugar pucker, glycosyl orientation, phosphodiester geometry, base pairing, base stacking, and the electrostatic environment of DNA phosphate groups. For both packaged and unpackaged states, the experiments were performed on aqueous solutions at 25 °C containing effective P22 DNA concentrations of 30–50 mg/mL in 200 mM NaCl + 10 mM $MgCl_2$ + 10 mM Tris at pH 7.5. At the experimental conditions employed, the B-form secondary structure of unpackaged P22 DNA is minimally perturbed by packaging the viral genome in the virion capsid. However, the electrostatic environment of DNA phosphates is dramatically altered with packaging. Specifically, we find the following: (1) C2′-endo sugar pucker and anti glycosyl orientations are conserved for all nucleosides. (2) Watson–Crick base pairing is essentially completely retained. (3) Alternative secondary structures, whether right- (A or C form) or left-handed (Z form), are not evident in either the packaged or unpackaged viral genome. (4) Small Raman hyperchromic effects (<10%) observed for certain marker bands of dG, dA, and dT in the packaged state of P22 DNA suggest slightly reduced base-stacking interactions with packaging. These are consistent with previously reported UV hyperchromic effects, but the Raman spectrum shows that they are not associated with either base unpairing or strand separation. (5) Marginal intensity changes within the envelope of the phosphodiester B-form Raman marker band (825–845 cm^{-1}) are consistent with a small net change in DNA groove dimensions attendant with packaging, interpreted as a net narrowing of the minor groove of B-form DNA, as has been observed for AT-rich sequences. (6) A large intensity decrease in the phosphodioxy Raman marker band with packaging is shown by analogy with model compounds to reflect increased electrostatic shielding of phosphates for the packaged genome. On the basis of model compound studies, the observed effect is judged to be equivalent to an approximate 10-fold increase in the local Mg^{2+} concentration in the packaged state of P22 DNA. (7) We find no evidence in the Raman spectrum of specific intermolecular interactions involving capsid protein and major-groove sites of packaged DNA. These findings apply both to wild-type P22 and to a mutant variant in which dsDNA of approximately 5% greater mass than wild type has been packaged. The present results, which appear to disfavor extensive folding, kinking, or sharp bending of the packaged P22 DNA, are discussed in relation to proposed models for organization of condensed viral chromosomes of dsDNA bacteriophages.

The dsDNA packaged in icosahedral viral capsids is highly condensed. In the case of the bacteriophage P22, the 43 400 base-pair genome is estimated to occupy a volume 10^3–10^4 smaller than that of uncondensed dsDNA in solution, and no proteins are bound along the DNA to hold it in this condensed state (Casjens, 1989). Low-angle X-ray diffraction measurements on P22 capsids and empty capsids indicate that the packaged DNA is a ball of uniform density with an outer radius of about 255 Å, inside a protein shell of mean radius 284 Å and approximate thickness 40 Å (Earnshaw et al., 1976). The density of the packaged P22 genome, which corresponds to about 0.9 g of DNA/g of H_2O (Casjens et al., 1992), is considered similar to that of oligomeric DNA in crystals and is sometimes compared to the condensed state of eukaryotic DNA in chromatin fibers (Serwer, 1989). The P22 diffraction results have been interpreted as evidence that most or all of the packaged DNA is in the B form (Earnshaw et al., 1976). The mean interhelix distance of packaged P22 DNA is approximately 28 Å, only 20% larger than the interhelix spacing in crystalline fibers of LiDNA at 66% relative humidity (Arnott, 1970).

A detailed model for dsDNA arrangement within the P22 capsid has been proposed by Earnshaw and Harrison (Earnshaw & Harrison, 1977; Harrison, 1983). According to this model, which is based primarily on the low-angle X-ray diffraction results, the dsDNA is characterized as a highly uniform, tightly wound, and concentrically layered "spool". The spool model appears to be consistent with electron micrographs obtained from gently disrupted capsids of dsDNA phages T3, T7, and λ (Richards et al., 1973; Earnshaw et al., 1978), although evidence which conflicts with the spool model has also been discussed for the case of phage λ (Haas et al., 1982; Widom & Baldwin, 1983). A distinguishing feature of the coaxially-wound DNA genome is the absence of significant numbers of sharp turns or kinks in the double helix and the prevalence of locally parallel arrays of double helices. Earnshaw and Harrison do not entirely exclude the possibility

† This is Part XXXVIII in the series Studies of Virus Structure by Laser Raman Spectroscopy, supported by NIH Grant AI11855.

* Author to whom correspondence should be addressed.
‡ University of Missouri—Kansas City.
§ University of Utah Medical Center.

0006-2960/92/0431-11835$03.00/0

of folds or kinks but confine them to plausible interaction sites between DNA and the capsid wall or to a central cavity of the spool which could contain up to 10% of the DNA in relatively sharply-folded arrays (Earnshaw & Harrison, 1977).

Black et al. have employed ion-etching of bacteriophage T4 to compare progressively eroded surfaces of the dsDNA packaged within the T4 virion capsid (Black et al., 1985). The ion-etching results have been interpreted in terms of a "spiral-fold" model for phage DNA packing. A distinguishing feature of the spiral-fold model is the substantial number of sharp (180°) bends occurring in the double helix along opposing faces of the capsid wall. A third model for phage dsDNA organization has been proposed on the basis of electron cryomicroscopy of T4 capsids (Lepault et al., 1987). The electron diffraction patterns of vitrified T4 samples appear to indicate locally ordered striations of DNA. These have been described as nematic liquid-crystalline domains of B-form DNA. Similar cryomicrographs have been obtained from vitrified samples of herpes simplex virus (Booy et al., 1991). Other biochemical and biophysical studies of dsDNA packaging in phage capsids have been reviewed (Black, 1988; Casjens, 1989; Serwer, 1989).

Up to the present it has not been possible to compare quantitatively the conformational properties of bacteriophage dsDNA in packaged and unpackaged states (Casjens, 1989). This reflects the experimental difficulties associated with probing the structure of the densely packed dsDNA molecule within the phage capsid. In previous work from this laboratory, preliminary Raman studies were reported on the packaged dsDNA of phages P22 (Thomas et al., 1982) and T7 (Thomas & Serwer, 1990). However, high-quality Raman spectra of mature capsids devoid of DNA and of the unpackaged, deproteinized genomic DNAs were not analyzed in those studies. Interpretation of the results was therefore limited to the essentially qualitative conclusion that the B form predominated over other possible DNA structural forms within the viral capsids.

More detailed structural features of the dsDNA packaged in virions, including those of P22, are not known. Although the data of low-angle X-ray diffraction and electron microscopy are consistent with dense packing of DNA having dimensions principally of the B form, the secondary structure of packaged dsDNA has not been probed quantitatively by a spectroscopic method sensitive to DNA conformation. Specifically, the nucleoside conformations and backbone phosphodiester geometry in the packaged P22 genome, and their distributions in comparison to those of unpackaged dsDNA, have not been determined directly. In principle, this information can be obtained from the Raman spectrum (Thomas & Wang, 1988). Additionally, it is now recognized that the B form of DNA is not a narrowly defined structure but a family of closely related structures exhibiting distinguishable differences depending upon the base sequence, the location and extent of bound water molecules, the ionic environment, and the presence of interacting proteins. [The structural polymorphism of B-DNA in the crystalline state and in cocrystalline protein complexes has been reviewed recently (Kennard & Hunter, 1989; Steitz, 1990).]

In the present work, we employ laser Raman spectroscopy to investigate the structure of the packaged P22 genome of wild-type phage capsids maintained in solution at conditions which preserve the native virion structure. For the first time, the data have been accurately compensated for the small but significant contributions made to the Raman spectrum by P22 capsid proteins. We have also conducted parallel Raman spectroscopic studies on protein-free P22 DNA molecules extracted from native phage capsids. We compare the Raman signatures with one another and identify genomic DNA subgroups which are structurally perturbed by packaging. The superior quality of the present spectral data, combined with the use of sensitive digital difference methods, permits structural characterization of essentially 100% of the packaged viral genome. The results obtained here establish the limits of B-form structure in packaged P22 DNA and provide new information relevant to proposed models of DNA organization in the phage capsid. The results obtained in this work also demonstrate the suitability of Raman spectroscopy for probing highly condensed states of dsDNA in native biological assemblies.

EXPERIMENTAL PROCEDURES

(1) Isolation and Purification of P22 Virions, Empty Capsids, and dsDNA. P22 virions, empty (DNA-free) capsids, and protein-free DNA were compared in this study. These different components were obtained using phages with nearly identical, but different, genotypes. The gene *c2* and *c1* mutations carried by some of the P22 strains below block lysogenization, and the *13⁻ am* mutation affects cell lysis. These mutations have no effect on virion structure, other than their single-base-pair changes in the DNA chromosome, and thus should have no effect on this study. (See Results and Discussion).

Virions were obtained from the isogenic strains P22 *c2⁻*H-5 *1⁻am*H201 (Botstein et al., 1973) and P22 *c2⁻*H-5 *1⁻*NT5/1 (Casjens et al., 1992). They were propagated on the *Salmonella typhimurium* host, strain DB7004, which carries a glutamine-inserting amber suppressor tRNA, so that infection by the *1⁻amber* mutant phage results in the production of a wild-type gene *1* protein (Eppler et al., 1991) and thus virions with completely wild-type proteins. The NT5/1 mutation changes one amino acid of the gene *1* protein and causes the encapsidation of chromosomes that are 5% longer than wild type within a normal-sized capsid (Casjens et al., 1992). Virions were purified as described (Earnshaw et al., 1976; Strauss & King, 1984). Empty capsids, prepared from lysates of host strain DB7136 (Prevelige et al., 1990) infected by P22 *c1⁻*7 *4⁻am*1368 *13⁻am*H101 (the kind gift of P. Prevelige and J. King), were purified as described by Strauss and King (1984). The gene *4* defect causes the accumulation of capsids which are missing the minor proteins encoded by genes *4*, *10*, *26*, and *9* [which make up 7–8% of the virion protein mass; those whose sequences are known (all but gene *26* protein) do not have unusual amino acid compositions (Eppler et al., 1991; Casjens et al., 1992)]. These capsids successfully encapsidate, but subsequently lose, their DNA (Lenk et al., 1976; Strauss & King, 1984).

Protein-free P22 DNA was obtained by phenol extraction of the P22 strain *c1⁻*7 *13⁻am*H101, which was propagated on host cells LT2 DB7136 (sup°) or LT2 DB7155 (sup⁺) (Prevelige et al., 1990). Water-saturated phenol was prepared by adding 20 mL of distilled, deionized water to approximately 10 g of freshly distilled phenol (BRL no. 5509UA, lot no. ANM205) and centrifuging the emulsion at 5000 rpm for 10 min to separate the phases. The top aqueous phase was discarded and the phenolic phase was adjusted to pH 7.5. A few milliliters of phenol solution was added to 10 mL of a solution containing approximately 10 mg of purified virions. After vortexing, the emulsion was allowed to separate and then vortexed again. This procedure was repeated several

times, followed by centrifugation at 11 000 rpm for 30 min to allow complete separation of the phases. The top aqueous phase was recovered, and to it were added 600 μL of sodium acetate at pH 6.2 and 20 mL of cold ethanol. The fibrous DNA was collected on a glass rod, washed several times with 3 volumes of cold ethanol, and evaporated to near dryness at 25 °C. The DNA was redissolved in distilled H_2O and dialyzed successively against several hundred volumes of 2 M NaCl + 1 mM EDTA (24 h), 0.5 M NaCl (24 h), and distilled H_2O (24 h), using 6000–8000 molecular weight cutoff SpectraPor dialysis tubing (Spectrum Medical, no. 132645). Following dialysis, the DNA solution was recovered, adjusted to pH 7.5, and lyophilized to near dryness. The lyophilysate was redissolved to 30–50 mg/mL in 200 mM NaCl + 10 mM Tris + 10 mM $MgCl_2$ (pH 7.5). The precise DNA concentration was determined by UV absorbance at 260 nm.

(*2*) *Preparation of Samples for Raman Spectroscopy.* Stock solutions of virions in 200 mM NaCl + 10 mM Tris + 10 mM $MgCl_2$, pH 7.5, were concentrated to approximately 80–100 mg/mL in a centrifugal microconcentrator (Amicon, Centricon) by means of low-speed sieving through a membrane with 10 000 MW cutoff. When the volume reached 200 μL, the solution was transferred to an Eppendorf tube and centrifuged at 8000 rpm for 30 min to pellet the phage. The supernatant was discarded, and 10-μL aliquots of the pellet were transferred to Kimax 34500 glass capillary tubes and sealed for use as Raman samples. The stock solution of empty capsids in 2.5 mM NaCl + 1 mM Tris + 0.2 mM EDTA, pH 7.1, was concentrated in a similar manner using a membrane of 30 000 MW cutoff. When the volume reached 125 μL, the solution was transferred to a calibrated Eppendorf tube and placed under a gentle N_2 stream until the final volume reached 15 μL, achieving an approximate 10-fold increase in concentration of both the empty capsids and buffer, as reported below. The sample was sealed in a glass capillary for Raman spectroscopy. The stock solution of P22 DNA, prepared as indicated above, was also sealed in a glass capillary for Raman spectroscopy. The sealed capillaries were mounted in a precision thermostat for data collection at 12 °C (Thomas & Barylski, 1970).

(*3*) *Instrumentation for Raman Spectroscopy.* Raman spectra were excited with the 514.5-nm line from an argon ion laser (Coherent Innova 70-4) using approximately 300 mW of power at the sample. The spectra were recorded on a Spex Model V/VI scanning spectrophotometer (Li et al., 1981). Data were collected at increments of 1 cm^{-1} with a spectral slit width of 8 cm^{-1} and integration time of 1.5 s. Spectra of P22 virions, empty capsids, and protein-free dsDNA were each collected and signal-averaged separately over the following three spectral intervals: 600–870, 870–1525, and 1500–1725 cm^{-1}. Extensive signal averaging, up to 30 scans, was carried out for each spectral region. Individual scans were examined for artifacts prior to averaging. Signal averaging was performed through ASYST routines.

(*4*) *Data Analysis.* For accurate comparison of spectra of packaged and unpackaged DNA and quantitative assessment of the spectral differences between them, the following protocol was followed for each of the three spectral regions 600–870, 870–1525, and 1500–1725 cm^{-1}. Thirty spectra of virions were collected and averaged to yield a spectrum of high signal-to-noise ratio corresponding to the DNA-filled phage capsid. Thirty spectra of the empty capsids were then collected and averaged to yield a spectrum of high signal-to-noise ratio corresponding to only the phage capsid proteins. The latter was subtracted from the former to yield by difference the spectrum of the packaged viral DNA. Finally, 30 spectra of the purified, protein-free P22 DNA were collected and averaged to yield a spectrum of high signal-to-noise ratio corresponding to the unpackaged dsDNA genome. The difference spectrum between the packaged P22 DNA (minuend) and the unpackaged P22 DNA (subtrahend) was then computed by direct subtraction. The positive and negative difference bands were measured from the flat baseline established by connecting the common points of zero Raman intensity (minima between bands) in the constituent spectra. Each band intensity change is expressed as the percentage change in the parent band intensity (minuend).

We also examined the difference spectra obtained after correction of the constituent spectra for the weak Raman contributions of the buffer solution. These were essentially identical to the difference spectra computed without corrections for the buffer solution, confirming that the observed spectral differences are due to structural changes in the viral components and not to baseline correction. Spectral subtractions, baseline corrections, and related data manipulations were performed using Spectracalc software.

In subtracting the spectrum of the empty capsids from the spectrum of the virion, the following bands were employed as primary standards for normalization of intensities: the 620-cm^{-1} band of phenylalanine, the 1003-cm^{-1} band of phenylalanine, and the 1551-cm^{-1} band of tryptophan. These normalizations led to no apparent bands of protein in the difference spectrum. This is expected, since the structure of the mature capsid is not altered by DNA removal (Prevelige et al., 1990, 1992). We have employed the following critera for significance of Raman difference bands. First, the difference feature should be apparent in the unrefined experimental data (i.e., in difference spectra computed from original data, uncorrected for baseline contours or solvent background). Second, the difference feature should not be greatly affected by baseline or solvent corrections. Third, a difference band should exhibit an intensity ratio at least twice that of the experimental noise level. Finally, the spectral feature must be reproducible for independently prepared samples.

RESULTS AND DISCUSSION

The complete Raman vibrational spectrum (300–3800 cm^{-1}) of aqueous P22 virions is compared with corresponding spectra of the empty capsids and isolated P22 DNA in Figure 1. The principal Raman bands and their residue assignments are given in Table I. This tabulation extends and refines earlier assignments (Thomas et al., 1982).

It is apparent from Figure 1 that the Raman spectrum of P22 virions is dominated by bands of the packaged DNA molecule. This is consistent with the weight percent compositions of protein (44%) and DNA (56%) in the virion (Casjens et al., 1992), and the fact that most Raman bands of DNA are intrinsically more intense than those of proteins (Thomas, 1987). Figure 1 shows also that the Raman signature of the packaged genome is remarkably similar to that of isolated P22 DNA. These spectra exhibit the characteristics noted previously for other aqueous dsDNA molecules of similar base composition (48% GC, 52% AT) (Prescott et al., 1984; Bamford et al., 1990), confirming the earlier conclusion that packaged P22 DNA is predominantly of the B form (Earnshaw et al., 1976; Thomas et al., 1982). However, despite these overall similarities, *the Raman spectra of packaged and unpackaged P22 DNA are not identical.* In order to better resolve the spectroscopic differences between

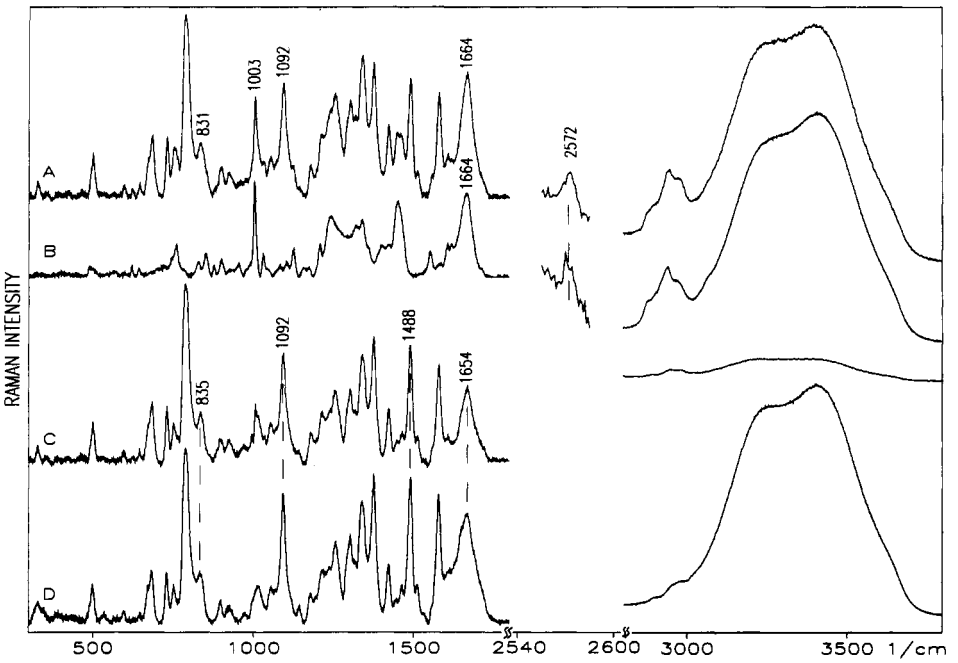

FIGURE 1: Comparison of the Raman spectrum of P22 virions with spectra of P22 protein and DNA constituents. (Left) Spectral region 300–1800 cm^{-1} of the native virion (A), the empty phage capsid (B), and their computed difference spectrum (C). The difference spectrum (C) identifies the Raman profile of the packaged P22 genome. Also shown is the Raman spectrum of the isolated P22 DNA molecules in H_2O solution (D). (Middle) Spectral region 2555–2585 cm^{-1} of native (top) and empty (bottom) phage capsids, showing the SH stretching band at 2572 cm^{-1} from the Cys405 residue of the capsid subunit (Eppler et al., 1991). DNA has no Raman bands in this spectral interval. (Right) Spectral region 2800–3800 cm^{-1} showing CH stretching bands of the native virion (A), empty phage capsid (B), packaged P22 DNA (C = B – A), and isolated P22 DNA (D). The OH stretching bands of the aqueous buffer, above 3000 cm^{-1}, dominate this region. Note that spectra C and D employ different baselines and solvent compensations, and therefore the contributed H_2O Raman intensities ca. 1640 (left panel) and above 3000 cm^{-1} (right panel) are not identical. Quantitative comparisons are given in Figures 2–4. Baseline procedures have been described previously (Aubrey & Thomas, 1991). All samples were at 12 °C and pH 7.5. Other experimental conditions are given in the text. Raman band frequencies and residue assignments are given in Table I.

packaged and unpackaged states of P22 DNA and to facilitate structural interpretations, we have applied extensive signal averaging to the contiguous spectral regions 600–870, 870–1525, and 1500–1725 cm^{-1}. The signal-averaged data are presented in Figures 2–4, which are discussed in turn.

(*1*) *The Spectral Interval 600–870 cm^{-1}.* The spectral region shown in Figure 2 contains DNA Raman bands which have been well characterized with respect to nucleoside conformation and backbone phosphodiester geometry (Thomas & Wang, 1988). The near superposability of the bands at 670 (dT), 681 (dG), 728 (dA), and 787 cm^{-1} (dC) in spectra of packaged (Figure 2C) and unpackaged (Figure 2D) states of P22 DNA indicates that C2′-endo sugar puckers and anti glycosyl orientations of nucleosides in the unpackaged state are conserved with packaging. Also, the absence of appreciable intensity changes or frequency shifts in conformation-sensitive bands of the dsDNA backbone (between 790 and 870 cm^{-1}) indicates conservation of the local B-form geometry of phosphodiester 5′C–O–P–O–C3′ linkages, including specifically the retention of 5′C–O and 3′C–O bond torsions, α and ζ in the gauche$^-$ and trans ranges, respectively (Benevides et al., 1988; Thomas & Wang, 1988).

The computed difference spectrum of Figure 2F (or Figure 2G) reveals, nonetheless, small but significant intensity differences between packaged and unpackaged states of DNA. The most clear-cut is the positive difference band near 681 cm^{-1} due to dG. This difference is attributed to a nominally lower intensity of the 681-cm^{-1} band of dG in unpackaged than in packaged P22 DNA (Table I). An analogous intensity difference occurs for the band assigned to dA at 728 cm^{-1}. The relative intensity changes in these marker bands of dG and dA are small (<10%) and, accordingly, represent rather small structural perturbations. The asymmetric shape of the dG difference band suggests as well a corresponding intensity change for the dT marker near 670 cm^{-1}. All of these features can be interpreted in terms of Raman hypochromism (Small & Peticolas, 1971); i.e., they represent larger Raman hypochromic effects in the unpackaged P22 DNA molecule and signify electronically greater interaction between stacked bases of unpackaged DNA. It is interesting to note that increased ultraviolet (UV) hypochromism has also been reported to accompany release of packaged T2 phage DNA (Tikchonenko et al., 1966). These authors interpreted the UV hyperchromicity of the packaged state as evidence of partial "disordering" of the T2 genome with packaging. An interpretation consistent with both the UV and Raman hyperchromicities of packaged DNA is given in Section 3 below.

In the region between 750 and 800 cm^{-1}, only marginal intensity changes are observed in the difference spectrum. These do not meet the criteria for significance defined above (Experimental Procedures), despite the fact that the parent 787-cm^{-1} band is the most intense in the DNA spectrum. However, the apparent absence of significant intensity change could be the result of cancellation of intensity perturbations of opposite sign, in the overlapping constituent bands due to dC (784 cm^{-1}) and the B-form backbone (ca. 790 cm^{-1}), which together generate the composite 787-cm^{-1} band. [For a review of DNA Raman band assignments, see Thomas and Wang (1988).]

Above 800 cm^{-1}, we observe a marginal positive difference band near 844 cm^{-1} and a marginal negative difference band near 828 cm^{-1}. These appear to represent an intensity shift from lower to higher frequency within the broad B-form backbone marker band, centered near 835 cm^{-1} in both packaged and unpackaged DNA (Table I). Such a frequency shift can be interpreted by analogy with Raman spectra of

Table I: Raman Frequencies and Assignments of P22 Virions, Empty Capsids, and DNA

virion[a]	empty capsid	unpkg. DNA	pkg. DNA	packaging sensitivity[b]	assignment	
					DNA[c]	protein[d]
	490			n		
499 (2.3)		499		n	dG, dT	
		535		n	dA	
596 (0.7)		597		n	dC, dG	
620 (0.4)	621			n		F
		646	638	n	dC, dA	
641 (0.8)	642			n		Y
670 (2.2)		669	670	n	dT, dG, dA	
681 (3.3)		680	681	y +9 ± 2	dG	
728 (3.4)		727	728	y +9 ± 2	dA	
	748			n		sc
753 (2.8)	758	750	750	n	dT, d	W
787 (10.0)		786	787	m[e]	dC, bk	
	829			n		Y
831 (2.9)		834	835	m[e]	bk	Y
	852			n		Y
	876			n		W
895 (1.7)	901	893	894	n	d	sc
921 (1.3)		919	920	n	d	
	954			n		sc
		972	972	n	d	
1003 (5.5)	1003			n		F
		1013	1014	n	d	W
1030 (2.0)	1031			n		F, sc
	1047			n		sc
1052 (2.3)		1054	1054	n	d	sc
	1081			n		sc
1092 (6.4)		1092	1092	y −24 ± 2	bk	
	1103			n		sc
1124 (1.8)	1125			n		sc
1143 (0.6)		1142	1143	n	dA, d	
	1157			n		sc
1178 (1.7)	1175	1178	1179	n	dT, dC	sc
	1208			n		Y, F, W
1210 (3.5)		1215	1216	n	dT	
		1237	1237	n	dT	
1238 (4.8)	1241			n	dT	AmIII
1254 (6.3)		1255	1255	n	dC, dA	
1302 (5.3)		1301	1302	n	dA	
1318 (3.7)	1320			n	dG	sc
1339 (7.9)	1340	1338	1339	y +7 ± 2	dG, dA	W, sc
	1358			n		W
1374 (7.5)		1374	1374	y −5 ± 2	dT, dA, dG	
	1402			n		sc
1420 (4.0)	1421	1420	1421	n	d	sc
		1444	1443	n	d	
1453 (3.6)	1451			n		sc
		1462	1462	n	d	
1488 (6.7)		1488	1488	y −4 ± 2	dG, dA	
1511 (1.5)		1511	1511	n	dA, dC	
1551 (1.3)	1551					W
			1553[f]			
1578 (5.9)	1581	1580	1578	n	dG, dA	W
1606 (2.4)	1606			n	dC	F
	1618			n		Y, W
		1655	1654	n	dT, dC, dG	
1664 (6.8)	1664			n	dT, dC, dG	AmI
2572	2572			n		C
2888	2878	2903	2892	n	d	sc
2940	2938		2952	n	d	sc
2974	2970	2981	2980	n	d	sc

[a] Raman frequencies are in cm^{-1} units. Intensities (in parentheses) are relative to the intensity (10.0) of the 787-cm^{-1} band. [b] Abbreviations: n = no significant sensitivity to packaging; m = marginal sensitivity; y = significant sensitivity. The percent intensity change between packaged and unpackaged states is given for bands marked y. Positive values indicate greater intensity in the packaged state. [c] Standard abbreviations are given for the nucleosides; bk = backbone vibration; d = deoxyribose vibration. More detailed assignments are discussed elsewhere (Lord & Thomas, 1967; Erfurth & Peticolas, 1975; Prescott et al., 1984). [d] One-letter symbols are given for aromatics and cysteine; sc = other side chain(s); Am = amide. Detailed assignments for many nonaromatic side chains are given elsewhere (Thomas et al., 1983). [e] See discussion in text. [f] Dissolved O_2.

polynucleotide fibers (Thomas et al., 1986) and oligonucleotide crystals (Benevides et al., 1988) as a change in groove dimensions of DNA. The present results suggest that packaged DNA exhibits, on average, a narrower minor groove than unpackaged DNA.

(2) *The Spectral Interval 870–1525 cm^{-1}.* The spectral region of Figure 3 contains a rich pattern of Raman bands due mainly to conjugated CC, CN, and CO stretching modes of the purine and pyrimidine bases. Also prominent is the 1092-cm^{-1} band, which is due to the symmetrical stretching

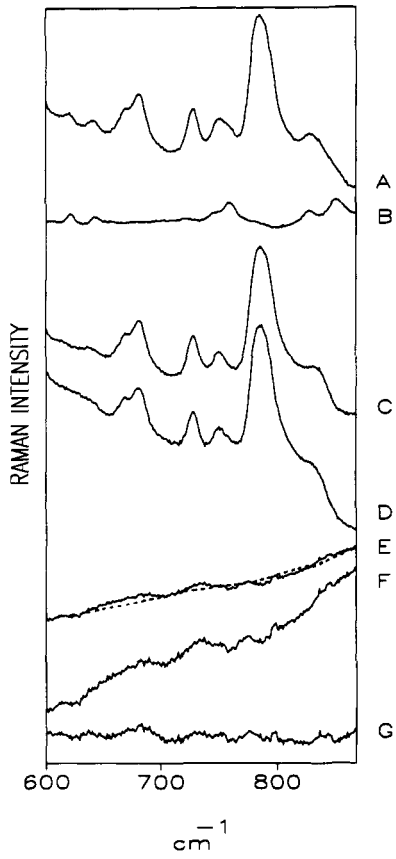

FIGURE 2: Signal-averaged Raman spectra in the region 600–870 cm^{-1} of the P22 virion (A), the empty phage capsid (B), the packaged P22 DNA (C = A – B), and the unpackaged P22 DNA (D). The computed difference spectrum between packaged and unpackaged states of P22 DNA is shown in E (= C – D) and amplified in F (= 2 × E). The baseline in trace E is indicated by a dashed line. Traces A through F represent experimentally recorded data, without baseline or solvent corrections. The DNA difference spectrum computed from solvent and baseline-corrected data is shown amplified 2-fold in G for comparison with F. All samples were at 12 °C and pH 7.5.

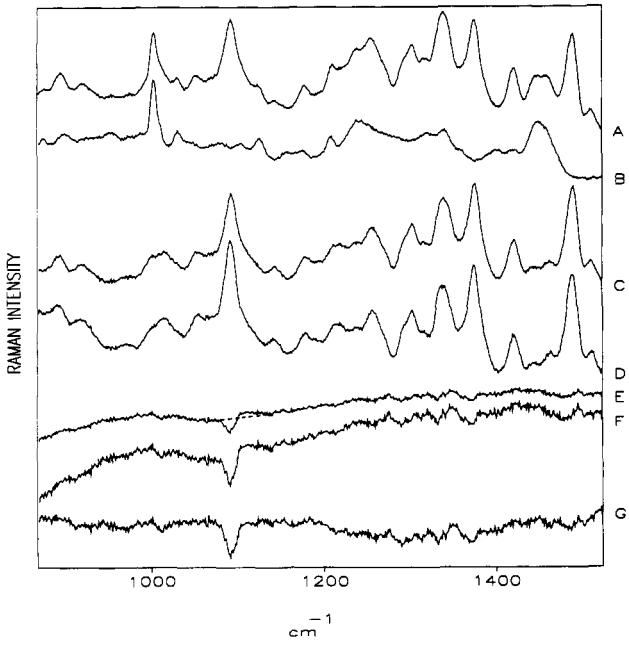

FIGURE 3: Signal-averaged Raman spectra in the region 870–1525 cm^{-1}. Traces are as described in the caption for Figure 2.

vibration of the phosphodioxy (PO_2^-) group of B-form DNA. This band exhibits a 24% intensity increase with unpackaging (or equivalently a 19% decrease with packaging), which is by

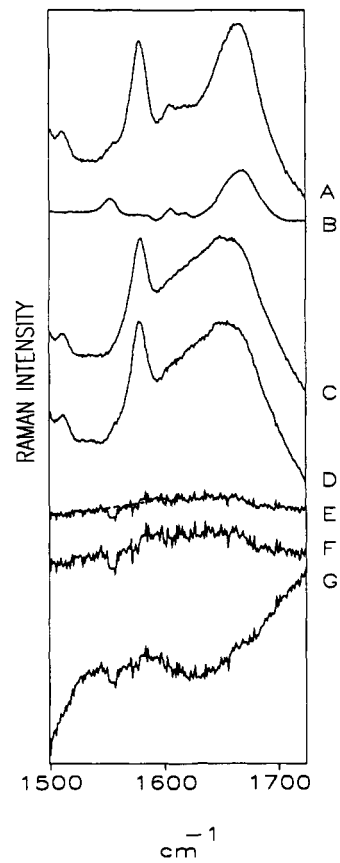

FIGURE 4: Signal-averaged Raman spectra in the region 1500–1725 cm^{-1}. Traces are as described in the caption for Figure 2. The negative difference band at 1553 cm^{-1} in traces E–G is due to O_2 (dissolved air) in the overcompensated solvent (see text). The water solubility of air at the experimental conditions employed corresponds to an effective O_2 molar concentration of $\approx 2.8 \times 10^{-4}$ M.

far the largest spectral difference between packaged and unpackaged states of the P22 genome. Interpretation of this result is straightforward. In the packaged DNA molecule, the PO_2^- groups are electrostatically shielded by high local concentrations of Mg^{2+}, which has the effect of reducing the polarizability change (i.e., Raman intensity) associated with the phosphodioxy symmetrical stretching vibration. Similar effects are noted for corresponding phosphate group Raman bands in spectra of alkyl phosphomonoester (Lord & Thomas, 1968) and phosphodiester salts of Mg^{2+} (K. L. Aubrey and G. J. Thomas, Jr., unpublished results). We show, for example, in Figure 5 that the effect of a 10-fold increase in Mg^{2+} cation concentration upon the Raman phosphodioxy symmetric stretching band of dimethyl phosphate anion is to reduce the band intensity by 25%. Note that the model compound difference band (Figure 5) is virtually identical in contour and intensity to the corresponding DNA difference band (Figure 3F). (The natural shape of the DNA difference band is preserved in Figure 3F but is slightly affected by the imposed baseline and solvent corrections of Figure 3G.)

Comparison of Figure 3 with Figure 5 allows the inference that the effective local Mg^{2+} concentration at phosphate groups is packaged P22 DNA is about an order of magnitude greater than that of unpackaged P22 DNA, even though bulk Mg^{2+} concentrations in the solutions from which they were prepared were identical. Further, the high local Mg^{2+} concentration in the phage is apparently essential to retention of its packaged DNA, as noted in the Conclusions section below.

The Figure 3E difference spectrum also reveals a small but significant negative difference band near 1374 cm^{-1}, indicating

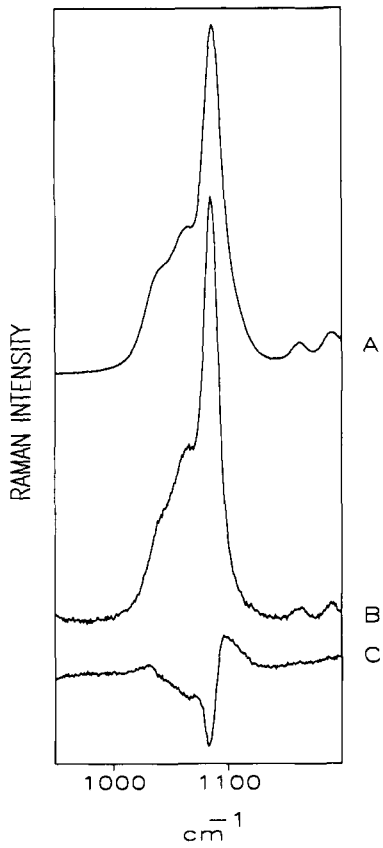

FIGURE 5: Raman spectra in the region 950–1200 cm^{-1} of magnesium dimethyl phosphate (MgDMP) in H_2O solution at 2.0 M (top) and 0.2 M (middle) and their difference spectrum (bottom). Data were obtained at 12 °C and pH 7.5. A similar difference spectrum resulted when the MgDMP concentration was fixed and the Mg^{2+} concentration was increased by addition of $MgCl_2$ (K. L. Aubrey and G. J. Thomas, Jr., unpublished results). Raman intensities in the minuend and subtrahend have been normalized to the intensity of the 757-cm^{-1} band (not shown), which exhibits no apparent band-shape dependence upon either ionic strength or electrolyte composition.

a net intensity reduction with packaging in the overlapping bands of dT, dA, and dG in this region. Because of the complex origin of the 1374-cm^{-1} difference band, a simple explanation cannot be given for its apparent net hypochromism with packaging. However, we find that the negative difference feature occurs at roughly twice the frequency (≈2×681) of the guanine difference marker discussed above. Accordingly, the possibility exists of a Fermi doublet coupling interaction (Herzberg, 1950). Similar complexities may apply to the marginal difference bands near 1340 (dA, dG) and 1490 cm^{-1} (dG, dA).

(*3*) *The Spectral Interval 1500–1725 cm^{-1}.* The spectral region of Figure 4 is dominated by an intense band at 1578 cm^{-1}, due to overlapping ring modes of dG and dA, and a broad complex band centered near 1654 cm^{-1}, due primarily to overlapping carbonyl (C=O) stretching vibrations of dT, dG, and dC. Adenine contributes no appreciable Raman intensity above 1600 cm^{-1} (Lord & Thomas, 1967). Additionally, the capsid subunits generate a moderately intense amide I band at ca. 1664 cm^{-1} (Figure 4B) which obviously contributes to the broad 1654-cm^{-1} band of the phage (Figure 4A) (Thomas et al., 1982). The unsubtracted spectra of Figure 4 (viz. Figure 4, traces A, B, and D) also contain contributing intensity between 1600 and 1680 cm^{-1}, due to the bending mode of solvent H_2O molecules. Because of somewhat different sample concentrations in the virion and empty capsid solutions, this solvent contribution is not completely canceled in the computation of the first difference spectrum corresponding to packaged P22 DNA (Figure 4C). Accordingly, in the computation of the second difference, between packaged and unpackaged DNA (i.e., Figure 4E), a residual contribution remains from solvent H_2O, which accounts for the observed broad and weak difference background between 1600 and 1680 cm^{-1}. Finally, we note that the absence of a positive difference band near 1578 cm^{-1} in Figure 4E confirms the fact that intrinsic hypochromicities of the purine ring modes near 1578 cm^{-1} are small in comparison to those of Raman bands in the 650–750- and 1200–1400-cm^{-1} intervals (Small & Peticolas, 1971; Erfurth & Peticolas, 1975).

Figure 4 also shows a barely discernible negative difference band at 1553 cm^{-1}. This band is extraordinarily sharp and cannot be attributed to any DNA or protein component of the phage. The nearby tryptophan band at 1551 cm^{-1} is much broader and is fully compensated by the first subtraction, which generates Figure 4C. This remarkable feature is due to the stretching vibration of O_2 (Herzberg, 1950) and originates from dissolved air in the aqueous samples. A corresponding N_2 stretching band of greater intensity at 2331 cm^{-1} is also detected in these solutions (data not shown). The appearance of the 1533-cm^{-1} band of O_2 in Figure 4E as a negative difference reflects subtraction of the spectrum of unpackaged DNA (Figure 4D, which has not been solvent-compensated) from the spectrum of packaged DNA (Figure 4C, which has been solvent-compensated by the first difference computation).

Detection of the O_2 Raman band in the Figure 4 difference spectrum provides an indication of the high sensitivity of the present spectral measurements. (See Figure 4 caption). Assuming that the intrinsic Raman cross section of the O_2 vibration is no greater than that of an intense Raman band of a DNA base vibration, such as the nearby purine 1578-cm^{-1} band, we would expect to detect intensity changes of the latter in the ≈300 μM range. This corresponds to a sensitivity for detection of relative intensity changes of about 0.5% in the parent 1578-cm^{-1} band. Since the latter is due to both dA and dG, the corresponding sensitivity per nucleotide type is approximately 1%.

Thus, the Raman difference spectrum between packaged and unpackaged states of P22 DNA contains no bands in the spectral region of Figure 4 which can be attributed reasonably to DNA. The essential identity of these spectra of packaged and unpackaged DNA indicates, importantly, that the carbonyl group interactions of the bases (dT, dG, and dC) are invariant to packaging. This result provides conclusive evidence that the base pairing of B-form DNA is unperturbed by packaging. Even small differences in the base-pairing content of DNA (Benevides et al., 1991a), or in the hydrogen bonding of guanine carbonyls to major-groove ligands (Benevides et al., 1991b), are known to yield significant band shifts in this spectral region.

(*4*) *Comparision of Wild-Type P22 and a Mutant Packaging 5% More DNA.* The spectroscopic protocols described above were repeated for the mutant P22 phage which packages a chromosome that is about 5% longer than wild type within a normal-sized capsid (Casjens et al., 1992). We obtained results on the packaged mutant genome which were indistinguishable from those described above for the packaged wild-type genome.

CONCLUSIONS

The principal conclusions of this study are that the B-form secondary structure of unpackaged P22 DNA is retained virtually completely with packaging in the phage capsid and that electrostatic shielding by Mg^{2+} of negatively charged

phosphate groups of packaged P22 DNA is about 10-fold greater than occurs for the unpackaged state. Although the B-form DNA backbone and base pairing are fully conserved, average groove dimensions and base stacking are altered slightly with packaging. These correlate well with other investigations (Tikchonenko et al., 1966; Benevides et al., 1991b,c; Bloomfield, 1991). We propose that the mode of packaging of DNA, whether in a concentric spool or spiral-fold configuration, is the source of the altered base-stacking interactions, which apparently generate both Raman and UV hyperchromic effects in packaged DNA states. The highly conserved (>98%) B-form structure of packaged P22 DNA is evidence that tertiary structure is also conserved. Models invoking gentle curvature of the double helix (Earnshaw & Harrison, 1977) would appear to be most consistent with the present results.

It would be difficult to reconcile the occurrence of substantial domains containing sharp folds, disordered single-stranded chains, or otherwise highly altered DNA backbones with the present results, since such perturbed structures would require more substantial departures from the B-form secondary structure of DNA. A simple spiral-fold model, for example, can be tested, albeit crudely, against the present results as follows. Assume the P22 capsid is a cube with 42-nm edges (approximately the same volume as the normal capsid but of different shape to simplify the calculation). A minimally folded genome of B-DNA might contain 3–4 disrupted base pairs per straight segment of 120 base pairs (42 nm ÷ 0.34 bp/nm) or not less than 2.5–3.5% non-B-form structure. The present results indicate that the admissible limit of non-B-form structure is less than 2%. A spiral-fold model with less than three disrupted base pairs (<6 nucleotides) per 120-bp segment of B-form DNA is not excluded by the Raman data.

ACKNOWLEDGMENT

We thank Dr. Peter E. Prevelige, Department of Biology, MIT, for generously providing purified samples of empty P22 phage capsids and for sharing expertise in the growth and isolation of bacteriophage P22 for Raman spectroscopy. The support of this research by Grant AI11855 (G.J.T.) of the National Institutes of Health is gratefully acknowledged.

REFERENCES

Arnott, S. (1970) *Progr. Biophys. Mol. Biol. 21*, 265–319.
Aubrey, K. L., & Thomas, G. J., Jr. (1991) *Biophys. J. 60*, 1337–1349.
Bamford, D. H., Bamford, J. K. H., Towse, S. A., & Thomas, G. J., Jr. (1990) *Biochemistry 29*, 5982–5987.
Benevides, J. M., Wang, A. H.-J., van der Marel, G. A., van Boom, J. H., & Thomas, G. J., Jr. (1988) *Biochemistry 27*, 931–938.
Benevides, J. M., Stow, P. L., Ilag, L. L., Incardona, N. L., & Thomas, G. J., Jr. (1991a) *Biochemistry 30*, 4855–4863.
Benevides, J. M., Weiss, M. A., & Thomas, G. J., Jr. (1991b) *Biochemistry 30*, 5955–5963.
Benevides, J. M., Weiss, M. A., & Thomas, G. J., Jr. (1991c) *Biochemistry 30*, 4381–4388.
Black, L. W. (1988) in *The Bacteriophages* (Calendar, R., Ed.) Vol. 2, pp 321–373, Plenum, New York.
Black, L. W., Newcomb, W. W., Boring, J. W., & Brown, J. C. (1985) *Proc. Natl. Acad. Sci. U.S.A. 82*, 7960–7964.
Bloomfield, V. A. (1991) *Biopolymers 31*, 1471–1481.
Booy, F. P., Newcomb, W. W., Trus, B. L., Brown, J. C., Baker, T. S., & Steven, A. C. (1991) *Cell 64*, 1007–1015.
Botstein, D., Waddell, C. H., & King, J. (1973) *J. Mol. Biol. 80*, 669–695.
Casjens, S. (1989) in *Chromosomes, Eukaryotic, Prokaryotic and Viral* (Adolph, K. W., Ed.) Vol. III, pp 241–261, CRC Press, Boca Raton, FL.
Casjens, S., Wyckoff, E., Hayden, M., Sampson, L., Eppler, K., & Randall, S. (1992) *J. Mol. Biol. 224*, 1055–1074.
Earnshaw, W. C., & Harrison, S. C. (1977) *Nature 268*, 598–602.
Earnshaw, W. C., Casjens, S., & Harrison, S. C. (1976) *J. Mol. Biol. 104*, 387–410.
Earnshaw, W. C., King, J., Harrison, S. C., & Eiserling, F. A. (1978) *Cell 14*, 559–568.
Eppler, K., Wyckoff, E., Goates, J., Parr, R., & Casjens, S. (1991) *Virology 183*, 519–538.
Erfurth, S. C., & Peticolas, W. L. (1975) *Biopolymers 14*, 247–264.
Haas, R., Murphy, R., & Cantor, C. (1982) *J. Mol. Biol. 159*, 71–92.
Harrison, S. C. (1983) *J. Mol. Biol. 171*, 577–580.
Herzberg, G. (1950) *Spectra of Diatomic Molecules*, 2nd ed., Van Nostrand, Toronto.
Kennard, O., & Hunter, W. N. (1989) *Q. Rev. Biophys. 22*, 327–379.
Lenk, E., Casjens, S., Weeks, J., & King, J. (1976) *Virology 68*, 182–199.
Lepault, J., Dubochet, J., Baschong, W., & Kellenberger, E. (1987) *EMBO J. 6*, 1507–1512.
Li, Y., Thomas, G. J., Jr., Fuller, M., & King, J. (1981) *Prog. Clin. Biol. Res. 64*, 271–283.
Lord, R. C., & Thomas, G. J., Jr. (1967) *Spectrochim. Acta 23A*, 2551–2591.
Lord, R. C., & Thomas, G. J., Jr. (1968) *Dev. Appl. Spectrosc. 6*, 179–199.
Prescott, B., Steinmetz, W., & Thomas, G. J., Jr. (1984) *Biopolymers 23*, 235–256.
Prevelige, P. E., Jr., Thomas, D., King, J., Towse, S. A., & Thomas, G. J., Jr. (1990) *Biochemistry 29*, 5626–5633.
Prevelige, P. E., Thomas, D., Aubrey, K. L., Towse, S. A., & Thomas, G. J., Jr. (1992) *Biochemistry* (in press).
Richards, K. E., Williams, R. C., & Calendar, R. (1973) *J. Mol. Biol. 78*, 255–259.
Serwer, P. (1989) in *Chromosomes, Eukaryotic, Prokaryotic and Viral* (Adolph, K. W., Ed.) pp 203–223, CRC Press, Boca Raton, FL.
Small, E. W., & Peticolas, W. L. (1971) *Biopolymers 10*, 69–88.
Steitz, T. A. (1990) *Q. Rev. Biophys. 23*, 205–280.
Strauss, H., & King, J. (1984) *J. Mol. Biol. 172*, 523–543.
Thomas, G. J., Jr. (1987) in *Biological Applications of Raman Spectroscopy*, Vol. 1, Raman Spectra and the Conformations of Biological Macromolecules (Spiro, T. G., Ed.) pp 135–201, Wiley-Interscience, New York.
Thomas, G. J., Jr., & Barylski, J. (1970) *Appl. Spectrosc. 24*, 463–464.
Thomas, G. J., Jr., & Wang, A. H.-J. (1988) *Nucleic Acids Mol. Biol. 2*, 1–30.
Thomas, G. J., Jr., & Serwer, P. (1990) *J. Raman Spectrosc. 21*, 569–575.
Thomas, G. J., Jr., Li, Y., Fuller, M. T., & King, J. (1982) *Biochemistry 21*, 3866–3878.
Thomas, G. J., Jr., Prescott, B., & Day, L. A. (1983) *J. Mol. Biol. 165*, 321–356.
Thomas, G. J., Jr., Prescott, B., & Benevides, J. M. (1986) *Biomol. Stereodyn. 4*, 227–254.
Tikchonenko, T. I., Dobrov, E. N., Velikodvorskaya, G. A., & Kisseleva, N. P. (1966) *J. Mol. Biol. 18*, 58–67.
Widom, J., & Baldwin, R. L. (1983) *J. Mol. Biol. 171*, 419–437.

Registry No. Mg^{2+}, 7439-95-4.